This is a preprint of the following article, which is available from `http://mdolab.engin.umich.edu`
J. T. Hwang, J. P. Jasa, and J. R. R. A. Martins. High-fidelity design-allocation optimization of a commercial aircraft maximizing airline profit. *Journal of Aircraft*, 2019.
The published article may differ from this preprint, and is available by following the DOI: `https://arc.aiaa.org/doi/abs/10.2514/1.C035082`.

High-fidelity design-allocation optimization of a commercial aircraft maximizing airline profit

John T. Hwang
University of California San Diego, La Jolla, CA 92093, United States

John P. Jasa and Joaquim R. R. A. Martins
University of Michigan, Ann Arbor, MI 48109, United States

Abstract

Traditionally, computational design optimization of commercial aircraft is performed by considering a small number of representative operating conditions. These conditions are based on the design Mach number, altitude, payload, and range for which the aircraft will be flown. However, the design also influences which routes and mission parameters are optimal, so there is coupling that is ignored when using the traditional approach. Here, we simultaneously optimize the aircraft design, mission profiles, and the allocation of aircraft to routes in an airline network. This is a mixed integer nonlinear programming problem that we reformulate as a nonlinear programming problem because of the large number of design variables. We solve the reformulated problem using a gradient-based optimization approach with a parallel computational framework that facilitates the multidisciplinary analysis and the derivative computation. We use a surrogate model for the CFD analysis that is re-trained in each optimization iteration given the new set of shape design variables. The resulting optimization problem contains over 4,000 design variables and close to 14,000 constraints. The optimization results show a 2% increase in airline profit compared to the traditional multipoint optimization approach. The wing area increases to the upper bound, enabling a higher cruise altitude that improves propulsive efficiency. We find that simultaneously optimizing the allocation, mission, and design to maximize airline profit results in a different optimized wing design from that resulting from the multipoint optimization approach.

1 Introduction

In the commercial aviation industry, there is significant interest in unconventional configurations as a means to meet aggressive targets for fuel burn, emissions, and noise reductions [1]. One of the challenges associated with designing these unconventional concepts is the lack of prior experience and data, which makes numerical simulation a valuable tool. With these applications, high-fidelity models are required because unconventional concepts exploit tight coupling between disciplines involving complicated physics, e.g., aeropropulsive coupling in concepts with boundary-layer ingestion and aeroelastic coupling in concepts with high-aspect-ratio composite wings. For these concepts, traditional empirical and low-fidelity models are insufficient to capture the dominant tradeoffs, even in a conceptual design setting.

When computational models become mature, efficient, and robust, applying numerical optimization can increase the value of the model in the design process. High-fidelity aerostructural optimization algorithms couple computational fluid dynamics (CFD) and finite-element analysis (FEA) to efficiently optimize the wing planform, section-wise airfoil shapes, and detailed structural sizing at the cost of only hundreds of simulations [2, 3]. Variants of this approach have been applied to the aerodynamic design of the blended wing body [4], truss-braced wing [5], and D8 [6].

The state-of-the-art approach in this field is multipoint fuel burn or drag minimization for aerostructural and aerodynamic optimization, respectively. The common approach is to minimize a weighted sum of fuel burn or drag values computed at a set of points sampled from a space consisting of Mach number, altitude, and lift coefficient (or alternatively, aircraft weight). These points, or operating conditions, are chosen for the design mission, representing the longest range the aircraft can fly. For aerostructural optimization, these on-design conditions are augmented with off-design conditions for maneuver load cases.

Given that the multipoint approach is now mature, we seek to evaluate the effectiveness of this approach compared to relaxing the 'multipoint' and 'design mission' assumptions. In this paper, we model the high-fidelity simulation using a surrogate model, allowing us to model (1) the full mission profile directly rather than a number of representative operating conditions and (2) the full set of missions in an airline network rather than just the design mission.

The primary motivation for this approach comes from the fact that many long-range airliners are flown well below their range. For instance, the Boeing 787's top five routes by seat capacity in Q3 2017 are all below 700 nmi [7], despite its range being between 6000-8000 nmi, depending on the variant. For short-haul routes, the operating conditions seen during climb and descent form a significant part of the flight, and they differ significantly from the cruise conditions of the long-haul mission. Therefore, a design optimization algorithm considering a set of operating conditions representing the long-range design mission is likely to produce a sub-optimal design. The secondary motivations for this full-mission, full-airline network approach include the evaluation of new concepts in terms of profit for the airline industry as well as the ability to model features that vary over the mission such as morphing wings and hybrid-electric propulsion systems. This new approach is more computationally demanding than the

multipoint approach, and it is only possible thanks to advances in computing hardware and algorithms as well as using the right combination of existing and new methods, which we later describe.

The objective of this paper is to develop this simultaneous allocation-mission-design optimization approach and apply it to the wing design of the common research model (CRM) [8]. Although part of the future motivation for this approach relates to unconventional configurations, we choose the CRM for this study because it has been extensively studied and hence there is significant data for the CRM. We use a 128-route hypothetical airline network and assume a fleet of existing aircraft based on an approximate, quarter-scale version of United Airlines' current fleet. This paper is an extension of work presented in a previous AIAA conference paper [9].

The coupled analysis of the allocation, mission, and design sub-problems can be summarized as follows. The design sub-problem consists of aerodynamic analysis using CFD, which is used to generate a surrogate model for lift and drag coefficient as a function of Mach number, angle of attack, and altitude. This surrogate model is used in the mission sub-problem to compute the operational profiles for 128 discretized missions. The mission analyses result in angle-of-attack, engine-thrust, and fuel-burn profiles at each of the 100 points that discretize the 128 missions. From the resulting data, the total fuel burn and block time values are evaluated for each mission, and this data is in turn used in the allocation sub-problem to compute the total profit and the allocation constraints.

The combined set of design variables consists of: wing area, sweep, twist distribution, and shape; the altitude profiles and cruise Mach numbers for the CRM on each of the 128 routes; and the allocation of the CRM in competition with the hypothetical airline's existing fleet of aircraft on the 128 routes. Each aircraft-route combination is parametrized with flights per day and passengers per flight. The objective function is profit, and there are constraints on the wing leading edge, thickness, volume, and moment coefficient; the climb angle, minimum thrust, and maximum thrust for each discretization point in the mission profiles; and the route demand and aircraft count in the allocation problem.

This paper is organized as follows. We start by presenting a literature survey and a description of our overall approach in Sec. 2. We then describe the methodology in Sec. 3, including both existing methods and methods that are new contributions. In Sec. 4, we describe the disciplinary models, which consist of aerodynamics, atmospheric models, the aerodynamic surrogate, the propulsion surrogate, aircraft dynamics, and airline allocation. We then present the problem in Sec. 5 and the optimization results in Sec. 6.

2 Background

In this section, we present literature surveys for high-fidelity design optimization and airline allocation. We then describe our approach in the context of the previous work in the relevant fields.

2.1 High-fidelity design optimization

High-fidelity optimization with respect to detailed aerodynamic shape and structural sizing variables is enabled by gradient-based optimization and the adjoint method. The adjoint method has been used for over four decades for aerodynamic [10] and structural [11] design optimization. The initial adjoint-based optimization approaches can be characterized as, what we now call, single-point optimization, where the flow or structural response is modeled and optimized at only one condition. It was quickly realized that this produces designs with low robustness—for instance, in 2-D transonic flow, the optimal airfoil shape is shock-free at the optimized Mach number, but away from it, drag increases significantly. Therefore, a multipoint approach was adopted as early as two decades ago in 2-D airfoil optimization as a way to prevent the optimizer from exploiting a large number of degrees of freedom [12, 13]. In the past decade, the multipoint approach has become routine, and it has been used for 3-D CFD-based aerostructural optimization of a Boeing 777-based model [3, 14], the D8 double-bubble configuration [6], a transonic wing with morphing trailing edges [15, 16], and a high-aspect-ratio tow-steered wing [17].

For purely aerodynamic optimization, the problem is typically formulated as a minimization of the drag coefficient subject to lift coefficient constraints at the various operating conditions. For purely structural optimization, the problem can be formulated as a compliance minimization or as a weight minimization subject to failure or tip deflection constraints. For aerostructural optimization, the objective function is typically fuel burn given a fixed range or range given a fixed fuel burn, as predicted by the Breguet range equation.

In multipoint fuel burn minimization, the points are typically based on a stencil in the shape of a grid or a cross, centered on a nominal condition in terms of some combination of Mach number, altitude, and weight or lift coefficient. The weights are most often selected using round numbers with higher weights closer to the nominal condition. Liem et al. [18] select the point locations and weights by performing mission analyses using the baseline design where the payload and range for each mission is determined based on real-world data. This approach addresses the limitation of the conventional multipoint approach, that it only designs for the design mission. However, it uses historical data, which limits predictive capability, and it does not capture the full allocation-mission-design coupling, since the multipoint weights are selected offline and the online portion is still a multipoint optimization.

In summary, all previous high-fidelity aircraft design optimization studies involving 3-D CFD formulate the objective function as a linear combination of a particular metric, evaluated at various operating conditions with different weights. The current work is unique because no such linear combination is used. Here, a finite number of high-fidelity evaluations are similarly utilized within each iteration, but rather than formulating the objective function directly from the outputs of the evaluations, we generate a surrogate model of the aerodynamic performance to enable direct modeling of full, discretized mission profiles.

2.2 Airline allocation

The allocation problem optimizes flights per day and passengers per flight for each aircraft and route combination as a way to determine on which routes to operate which aircraft, emulating a profit-seeking airline. By itself, it is a linear programming problem. The airline allocation problem has been studied since the 1950s [19]; thus, it was one of the first applications of the simplex method, which was developed in 1947 [20]. In the 1960s, researchers started using optimization for flight scheduling [21] and later, the fleet assignment problem (FAP)—determining the optimal allocation of aircraft to scheduled flights—using linear programming for problems of realistic sizes [22]. Research in the past decade has focused on improvements such as better revenue models [23, 24] and simultaneously performing scheduling and fleet assignment [25]. The FAP algorithms have had a practical impact on airline operations [22, 26, 27].

Several recent research efforts have investigated the idea of simultaneously designing a new aircraft and solving the fleet allocation problem. The early studies formulated the problem as a mixed-integer nonlinear programming (MINLP) problem with profit as the objective function [28, 29]. Mane et al. [28] and Marwaha and Kokkolaras [30] use decomposition-based approaches that iteratively solve the allocation problem and the aircraft sizing problem separately, which enables better scalability than a general-purpose MINLP solver, since the mixed-integer part is contained in the linear allocation problem. Others have focused on developing new MINLP algorithms based on an efficient global optimization approach [31, 32, 33]. Another area of focus has been robust design-allocation optimization given uncertain passenger demand [34, 35].

The two primary differences between the previous work and the current work are that: (1) the previous efforts use low-fidelity aircraft models, whereas we use 3-D CFD, which enables detailed shape optimization; and (2) we treat the integer design variables—flights per day—as continuous variables. The latter assumption is made with the rationale that the focus is on the wing design obtained through optimization. While treating the variables as integers is likely to result in small changes to the optimal fleet allocation, it is not expected to have a large impact on the optimal wing design.

The current work represents the culmination of a series of previous efforts building towards high-fidelity design-allocation of a large representative airline network. The first effort demonstrated allocation-mission optimization with a 3-route network [36] using a mixed-integer optimization algorithm, follow-up work performed allocation-mission optimization with a 128-route network using parallel computing with relaxed integrality constraints [37], and later work extended this to allocation-mission-design optimization using Euler-based CFD [9].

In this paper, we perform allocation-mission-design optimization with the same 128-route network using a Reynolds-averaged Navier–Stokes (RANS) CFD solver. We build upon the prior allocation-design optimization work [9] by using a more relevant geometry (the CRM) as well as more realistic models.

3 Methodology

3.1 Overall Approach

In this paper, we develop a RANS CFD-based simultaneous allocation-mission-design optimization approach. We use this approach to design a next-generation aircraft—based on the CRM—for a market with 128 routes and an existing aircraft fleet modeled as a quarter-scale version of the United Airlines fleet. The design variables consist of almost 200 wing design variables (area, sweep, twist distribution, and airfoil shapes), the CRM's discretized altitude profiles and cruise Mach numbers for the 128 routes, and the flights per day and passengers per flight for each route and each aircraft type in the fleet. We generate surrogate models of the aircraft performance using RANS CFD training data, and these surrogate models are used to perform mission analyses for the 128 routes and compute fuel burn and flight time values. This data is then used to compute profit and the relevant constraints in the allocation model. The objective function being maximized is profit.

From the airline's perspective, this approach is a way to gain insight into the most profitable aircraft design given their current routes and fleets. Alternatively, from the aircraft manufacturer's perspective, this approach is a tool for designing a profitable next-generation aircraft given the current routes and fleets of the industry as a whole. While many limitations remain that detract from these goals, these potential applications for airlines and aircraft manufacturers provide the long-term motivation for the proposed approach of simultaneously optimizing the design and allocation.

The multidisciplinary model components is shown in Fig. 1 as an extended design structure matrix [38]. The overall strategy is to solve the optimization problem as a nonlinear program (NLP) using the multidisciplinary feasible (MDF) architecture, where nonlinear and linear block Gauss–Seidel solvers are used to fully converge the coupling in the model [39]. As Fig. 1 illustrates, the optimizer passes design variables into the overall model, and this model computes the constraints as well as the objective function (profit), which are fed back to the optimizer. The coupling between the aerodynamic surrogate, propulsion surrogate, and mission equation blocks is handled in the mission analysis discipline (Sec. 4.6).

The remainder of this section describes the methods used to solve the simultaneous allocation-mission-design optimization problem in an efficient way. We do so by presenting the methods as solutions to four computational challenges: high-dimensional optimization, model complexity, large cost of CFD, and optimization convergence. The solutions to the first two challenges use previously developed methods; those for the last two challenges represent new contributions.

3.2 Challenge 1: high-dimensional optimization—adjoint approach

The first challenge is the large number of design variables in the optimization problem. There are about 200 design variables that parameterize the wing shape, about 2600 that parametrize the 128 altitude profiles, and about 1300 allocation variables, resulting in a total of over 4100 design variables.

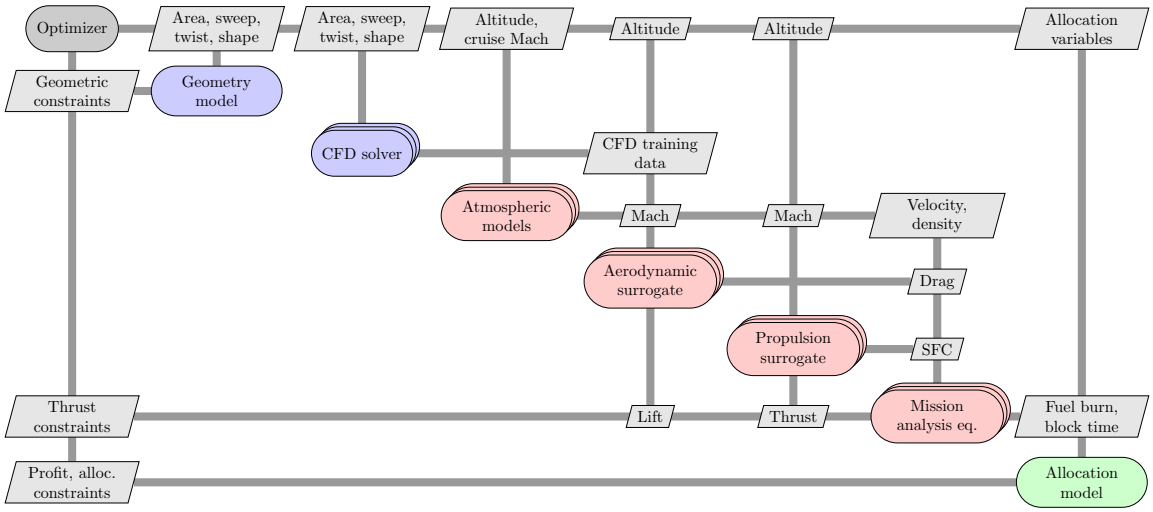

Figure 1: Design structure matrix showing the design (blue), mission (red), and allocation (green) parts of the model and the dependencies between them.

We are able to solve this high-dimensional optimization problem thanks to a combination of a gradient-based optimization algorithm with an adjoint approach that efficiently computes the required gradients. We use the multidisciplinary feasible (MDF) architecture [40, 39], where a single monolithic optimizer is used to solve the problem and the model resolves all feedback loops with solvers. The gradient-based optimizer is SNOPT [41], which uses a robust sequential quadratic programming algorithm that is efficient for problems with large numbers of design variables and constraints. We compute the derivatives of the objective function and constraint functions using the adjoint method [42, 43], since it can compute accurate derivatives and its cost is practically independent of the number of design variables in models with coupling.

3.3 Challenge 2: model complexity—modular approach

The second challenge is dealing with the complexity of the model. Since we are using the MDF approach, we develop a single model that integrates the CFD analyses, allocation models, and 128 mission analyses, which includes propulsion, aircraft dynamics, an ordinary differential equation (ODE) that computes the fuel burn over the mission, and the aerodynamic-performance surrogate model. These sub-models are parallelized differently, and the use of the adjoint method imposes additional requirements and difficulties in developing the integrated model.

To simplify the model development, we take a modular approach and use NASA's OpenMDAO (open-source multidisciplinary design, analysis, and optimization) software framework [44]. OpenMDAO is a framework for solving multidisciplinary design optimization (MDO) problems that supports efficient derivative computation using the modular analysis and unified derivatives (MAUD) architecture [45]. In OpenMDAO, a model is implemented in a modular way as a set of *Component* objects with a consistent interface that are hierarchically and recursively combined using *Group* objects.

The MAUD architecture uses a generalization of the adjoint method [46, 47]. MAUD works with any combination of components defined by implicit or explicit functions, whereas the adjoint method requires a particular type of model where implicit functions define the states and explicit functions define the functionals. The chain rule naturally falls out of this generalization if the model has only explicit functions that depend sequentially on each other.

MAUD simplifies derivative computation in complex heterogeneous models because regardless of the model structure, there are always two steps: computing the partial derivatives and computing the total derivatives by solving a linear system. For our model, we compute the partial derivatives using hand-differentiation everywhere except for the CFD solver—there, we use the CFD solver's native adjoint solver [42, 43]. The total derivative computation consists in solving a linear system with a right-hand side for each objective or constraint function for which we require derivatives.

3.4 Challenge 3: large cost of CFD—dynamically trained surrogate model

The third challenge is that tens of millions of evaluations of the aerodynamic model are required, which is not feasible in a reasonable amount of time with a CFD model. The aerodynamic model must be evaluated at each of the $\mathcal{O}(100)$ points in each mission analysis, and the coupling in the mission equations necessitates a solver that requires $\mathcal{O}(10)$ iterations. Compounding on this, there are 128 missions, and the optimizer requires $\mathcal{O}(100)$ iterations. Combining all of these factors results in at least tens of millions of evaluations of the aerodynamic model.

Since tens of millions of RANS CFD evaluations would be prohibitively expensive, we replace the CFD model with a surrogate model. A surrogate model in terms of the hundreds of wing design parameters would also require a prohibitively large amount of CFD evaluations to train. Therefore, we use a surrogate model whose only inputs are the parameters that represent the operating condition—Mach number, angle of attack, and altitude. Since the training data for the surrogate model changes as the wing design parameters change, the surrogate model is re-trained in each optimization iteration, given the CFD training data computed from the current iterates for the wing design parameters. However, since we are taking a gradient-based approach, this means that we require derivatives of the surrogate model's outputs with respect to not only the inputs, but also the training data.

A surrogate model can be generally formulated as

$$y = f(x, x_t, y_t), \tag{1}$$

where x_t is the vector of training point inputs, y_t is the vector of training point outputs, x is the prediction input vector, and y is the prediction output. Derivatives are often relevant in surrogate modeling; gradient-enhanced surrogate models take dy_t/dx_t as additional training data and evaluating derivatives at prediction points consists in computing dy/dx. However, here, the derivatives with respect to training data that we are referring to are dy/dy_t.

The need for dy/dy_t presents a unique requirement that motivated the development of a new surrogate model called regularized minimal-energy tensor-product splines (RMTS) [48]. RMTS interpolates the training data with tensor-product cubic Hermite splines or B-splines and solves an optimization problem that minimizes energy while approximating the training points. RMTS is designed so that the prediction outputs are differentiable with respect to the training outputs, and so that these derivatives can be readily computed.

3.5 Challenge 4: optimization convergence—single-discipline pre-optimizations

The final challenge is dealing with potentially slow optimization convergence due to the large number of dimensions and disciplines. Since SNOPT is a quasi-Newton algorithm, the Hessian matrix is initialized to the identity matrix and is gradually updated throughout the optimization. With over 4000 design variables, it can take hundreds of iterations for the Hessian approximation to become adequate to achieve second-order convergence rates. Moreover, the presence of design variables from many disciplines makes scaling a challenge. It is difficult to choose the right scaling parameters for the design variables to avoid situations where the optimizer largely neglects to change certain design variables until after tens of optimization iterations.

We address these issues by pre-optimizing each part of the larger MDO problem on its own and extracting the initial design variable values from those results. Specifically, we perform a multipoint design optimization, followed by 128 separate mission optimizations, followed by an allocation optimization. The multipoint design optimization provides initial values for the wing design variables in the full MDO problem. Based on the resulting design, an initial aerodynamic surrogate model is generated, which is used to perform the 128 mission optimizations with a fixed wing design to provide initial altitude profiles for the full MDO problem. Using the fuel burns and block times computed from these mission optimizations, a pure airline allocation optimization is performed to obtain an initial values for the allocation design variables in the full MDO problem. This allocation optimization also provides a baseline profit value for the multipoint approach. This value provides a point of reference for measuring the profit improvement achieved by the allocation-mission-design optimization.

4 Models

4.1 Geometry model

The geometry of interest is the Common Research Model (CRM) wing [8, 49]. We use the high-fidelity aircraft design optimization tool suite developed by Kenway and Martins [2]—MDO of aircraft configurations with high-fidelity (MACH). In this approach, the discrete representation of the CRM is parametrized using a free-form deformation volume where the volume is a 4th order tensor-product B-spline [49]. This is illustrated in Fig. 2. There are two relevant maps: the wing area, sweep, twist, and shape design variables first map to the B-spline control point coordinates (shown in red in Fig. 2),

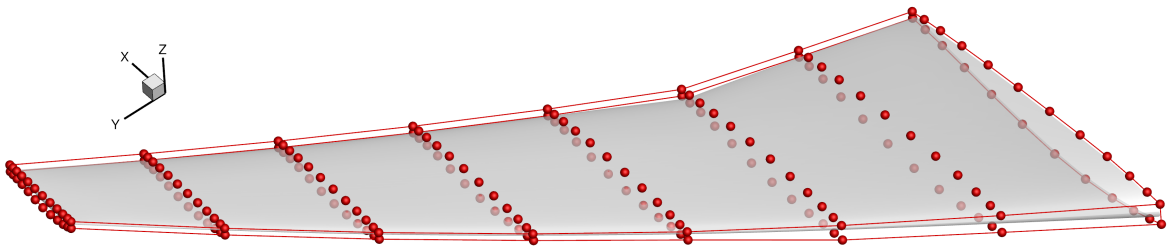

Figure 2: The Common Research Model (CRM) wing [51] enclosed in a free-form deformation block with the control points shown in red.

and the B-spline control point coordinates map to the new surface nodes. The first map is differentiated using the complex-step method [50], and the second map is linear and the partial derivative Jacobian is simply the matrix representing the mapping.

From the surface nodes, we compute thickness and volume constraints, as we show in Fig. 1. The computation of these constraints given wing area, sweep, twist, and shape is implemented as a single OpenMDAO component—the internal details of the FFD mapping and the associated derivative computation are abstracted from OpenMDAO and are all handled within the MACH framework.

4.2 CFD solver

The CFD solver we use, ADflow, is also part of the MACH framework. ADflow is a structured multi-block finite-volume solver with multigrid [2]. ADflow solves the Reynolds-averaged Navier–Stokes (RANS) equations using the fourth-order Runge–Kutta scheme or the diagonally dominant alternating direction implicit (DDADI) scheme, combined with the Newton–Krylov method. Derivatives of the functionals with respect to geometric design variables are computed using the adjoint method with partial derivatives computed using algorithmic differentiation.

The CFD mesh deformation algorithm we use propagates the displacements and rotations from the deformed surface to the full CFD volume mesh by using inverse-distance weighting [52]. More specifically, the deformation of each node in the CFD volume mesh is the sum of the displacements and rotations of all the nodes on the deformed surface, weighted by the inverse of the distance to that surface node.

In the context of the model in Fig. 1, the OpenMDAO component for the CFD solver computes lift and drag coefficients as a function of wing area, sweep, twist, and shape. The outputs are used to train a surrogate model in terms of Mach number, angle of attack, and altitude. Therefore, each instance of this CFD solver component is assigned a fixed Mach number, angle of attack, and altitude that does not change throughout the optimization. Using the MAUD architecture, OpenMDAO automatically parallelizes across these instances and the CFD solver also internally runs in parallel. There are 36 training points, and we run with 140 processors in total, so each training point is computed using 3 or 4 processors.

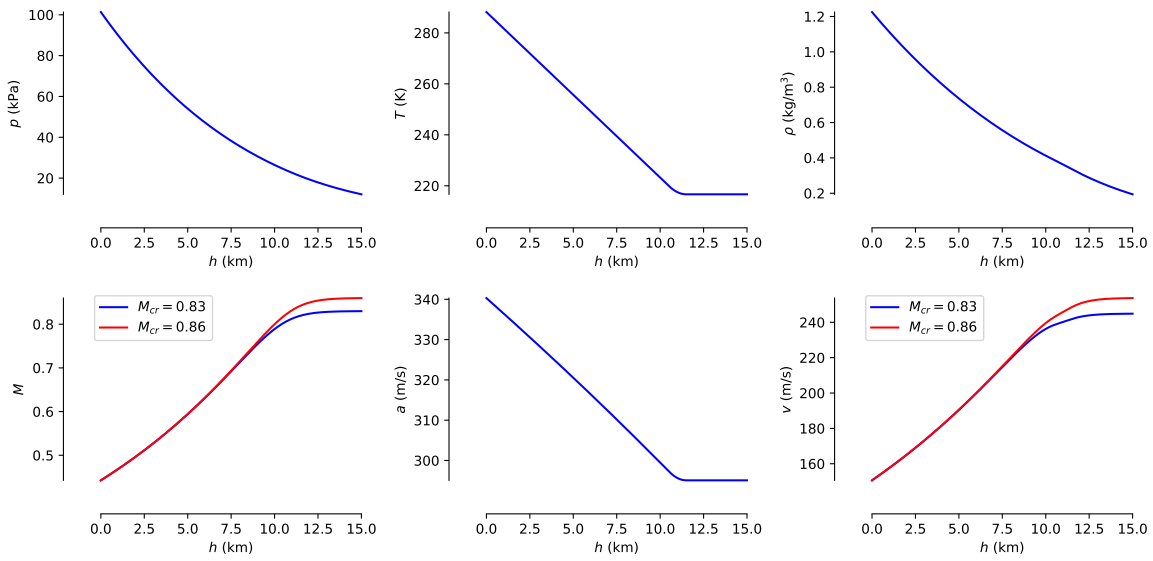

Figure 3: Pressure, temperature, density, and speed of sound are computed using atmospheric models. For the Mach number, we assume a constant indicated airspeed climb at 300 knots until the cruise Mach number is reached.

4.3 Atmospheric models

In this section, we describe the computation of various altitude-dependent quantities that are required for mission analysis. OpenMDAO components are implemented to compute each of the quantities shown in Fig. 3 in a vectorized manner—the values at all mission points are vectorized and computed together for efficiency.

Temperature, pressure, density, and speed of sound. The dependence of temperature on altitude is assumed to be linear in the troposphere and constant in the stratosphere—the effects of local weather conditions are not considered. The tropopause, the boundary between the troposphere and stratosphere, depends on the latitude and the local atmospheric conditions, but we approximate it to occur at 11 km everywhere. Since we require smooth derivatives, we use a cubic function to smoothly transition between the linear and constant regions. Temperature as a function of altitude is given by

$$T(h) = \begin{cases} T_0 - L \times h, & h < h_t - \epsilon \\ c_3 h^3 + c_2 h^2 + c_1 h + c_0, & h_t - \epsilon \leq h \leq h_t + \epsilon \\ T_1, & h_t + \epsilon < h \end{cases} , \tag{2}$$

where $T_0 = 288.16\,\mathrm{K}$ is the temperature at sea level, $T_1 = 216.65\,\mathrm{K}$ is the temperature in the stratosphere, $L = 6.5\,\mathrm{K/km}$ is the lapse rate, $h_t = 11\,\mathrm{km}$ is the tropopause altitude, and $\epsilon = 0.5\,\mathrm{km}$ is the half-width of the smoothing region. The cubic function coefficients are given in Appendix A.

Pressure is computed by integrating the hydrostatic equation, replacing density with an expression involving pressure and temperature using the ideal gas law. Since we know that temperature is linear and constant in the troposphere and stratosphere, respectively, we can insert the known functions and analytically solve for pressure as a function of altitude. We end up with different functions in the two regions, and we smooth the transition using a cubic function as before. Pressure as a function of altitude is given by

$$p(h) = \begin{cases} p_0 \left(\frac{T(h)}{T_0}\right)^{\frac{g}{LR}}, & h < h_t - \epsilon \\ d_3 h^3 + d_2 h^2 + d_1 h + d_0, & h_t - \epsilon \leq h \leq h_t + \epsilon \\ p_1 \exp\left(\frac{g(h_t - h)}{RT_1}\right), & h_t + \epsilon < h \end{cases}, \tag{3}$$

where $p_0 = 101325\,\text{Pa}$ is the pressure at sea level, $p_1 = 22632\,\text{Pa}$ is the pressure in the stratosphere, $g = 9.81\,\text{m/s}^2$ is the acceleration due to gravity, and $R = 287\,\text{m}^2/\text{s}^2/\text{K}$ is the gas constant. The cubic function coefficients are given in Appendix B. Given the temperature and pressure, we can easily compute density from the ideal gas law using

$$\rho = \frac{p}{RT}, \tag{4}$$

and the speed of sound using

$$a = \sqrt{\gamma RT}, \tag{5}$$

where $\gamma = 1.4$ and again, $R = 287\,\text{m}^2/\text{s}^2/\text{K}$.

Mach number and true airspeed. In the optimizations involving mission analysis, we allow cruise Mach number to be a variable, and the Mach number profile over the mission is uniquely determined by the cruise Mach number and altitude profile. The idea is that we assume a constant indicated airspeed (IAS) of 300 knots when below a critical altitude and switch to a constant Mach number (the specified cruise Mach number) during cruise. More precisely, we compute the true airspeed (TAS) corresponding to an IAS of 300 knots at all points and use the lower of this value and the value computed from the specified cruise Mach number. However, instead of using the minimum function, we use the Kreisselmeier–Steinhauser [53] function since we require a smooth minimum.

We now develop the relationship between IAS and TAS using the known and measured total pressure. IAS is the value shown to the pilot on the airspeed indicator and is measured via impact pressure, $q_c = p_t - p$. Since local air density cannot be measured, IAS is computed from impact pressure using the sea-level density, ρ_0. Therefore, total pressure as a function of IAS is

$$p_t = p + \frac{1}{2}\rho_0 v_{\text{IAS}}^2. \tag{6}$$

TAS is the true airspeed that can be used to compute the Mach number. Total pressure as a function of TAS is given by

$$p_t = p\left[1 + \frac{\gamma - 1}{2}\left(\frac{v_{\text{TAS}}}{a}\right)^2\right]^{\frac{\gamma}{\gamma-1}}. \tag{7}$$

Combining these two expressions for total pressure and inserting $\gamma = 1.4$, we obtain

$$v_{\text{TAS}} = a\sqrt{5}\sqrt{\left(\frac{\frac{1}{2}\rho_0 v_{\text{IAS}}^2}{p} + 1\right)^{\frac{2}{7}} - 1}. \tag{8}$$

4.4 Aerodynamic surrogate model

The aerodynamic surrogate model maps Mach number, angle of attack, and altitude to the lift and drag coefficients. As mentioned previously, the surrogate model is necessary because tens of millions of aerodynamic evaluations are required due to: the discretization of the 128 mission profiles, the iterations required for converging the mission equations, and the iterations solving the optimization problem. We use the aforementioned RMTS interpolant, which meets our requirement for derivatives with respect to training data.

In Fig. 4, we show the training point locations and investigate the accuracy of the surrogate. Among the three input variables, Mach number M and angle of attack α are the most of interest; altitude is less important because of the aforementioned relationship between Mach number and altitude. We cannot neglect altitude completely as a third input variable because cruise Mach number is not known a priori. Instead, we sample in the $M-\alpha$ space as shown in the right-hand plots in Fig. 4 and for each of the 18 points in the $M-\alpha$ space, we sample at two altitudes close to the one suggested by the bottom left plot in Fig. 3. Therefore, we have 36 training points in total.

In the $M-\alpha$ space, we choose the distribution shown in Fig. 4 because we know that the lift and drag coefficients have more nonlinearity versus M than versus α. The left and center plots in Fig. 4 confirm this; lift and drag coefficient show low curvature versus α, but drag coefficient varies significantly with M because of the well-known drag bucket and drag divergence. Moreover, we know that as M decreases, altitude decreases, and α increases. Therefore, accuracy is required neither at low M and low α nor at high M and high α. Given this unstructured distribution of points, RMTS interpolates the data smoothly with an interpolation error that is less than 0.2% for the data set shown in Fig. 4, and the surrogate model follows the general trends, as required. As the optimization proceeds, the training outputs change for the 36 points, but the locations of the points in M-α-h space are held fixed, where h is altitude.

4.5 Propulsion surrogate model

The propulsion surrogate model maps Mach number, altitude, and throttle to thrust and thrust-specific fuel consumption (SFC). The surrogate model uses data from the Numerical Propulsion System Simulation (NPSS) [54] engine cycle analysis tool for a GE-90-sized engine. Again, RMTS is used to interpolate the data, which is structured in this case. In Fig. 5, we plot 1-D slices of both thrust and SFC with respect to all three input variables. The plots confirm that the surrogate model captures the trends and approximates the training data with minimal interpolation error and without introducing spurious oscillations.

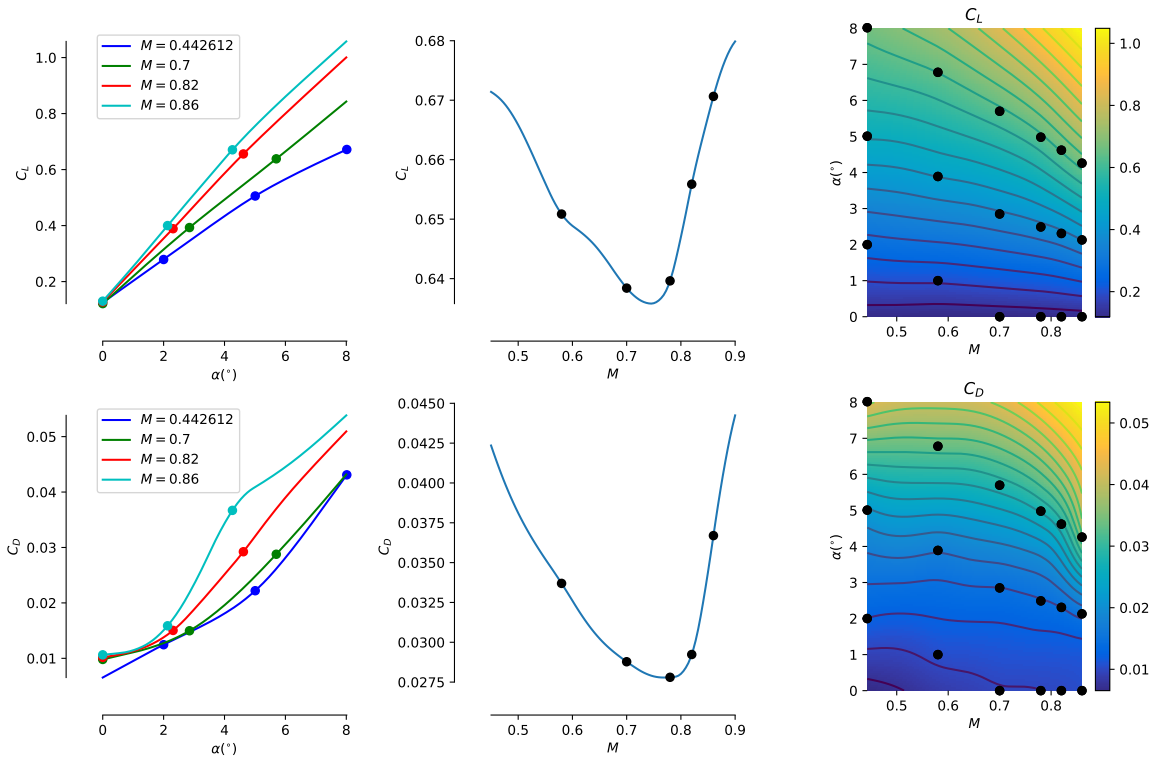

Figure 4: 1-D slices and contour plots for the aerodynamic surrogate model for the CFD solver. The plots in the middle represent a diagonal slice passing through the top row of training points in the contour plot.

4.6 Mission analysis equations

In this section, we describe the vertical and horizontal equations of motion, the fuel weight ordinary differential equation (ODE), the method of solving the ODE, and the solver for the coupled system.

The vertical and horizontal equations of motion are aligned with the freestream velocity direction, and they are given by

$$T\cos\alpha - D - W\sin\gamma - \frac{W}{g}\dot{v}_y\sin\gamma - \frac{W}{g}\dot{v}_x\cos\gamma = 0, \tag{9}$$

$$T\sin\alpha + L - W\cos\gamma + \frac{W}{g}\dot{v}_x\sin\gamma - \frac{W}{g}\dot{v}_y\cos\gamma = 0, \tag{10}$$

where T, L, D, and W are the total aircraft thrust, lift, drag, and weight, respectively, α is the angle of attack, γ is the climb angle, and $\dot{v}_x$ and $\dot{v}_y$ are the horizontal and vertical components of acceleration in the Earth-fixed frame. While these equations can be interpreted as an ODE, we have a guess for the altitude profile coming from the optimizer, so we use these equations to solve for and compute thrust and lift, respectively.

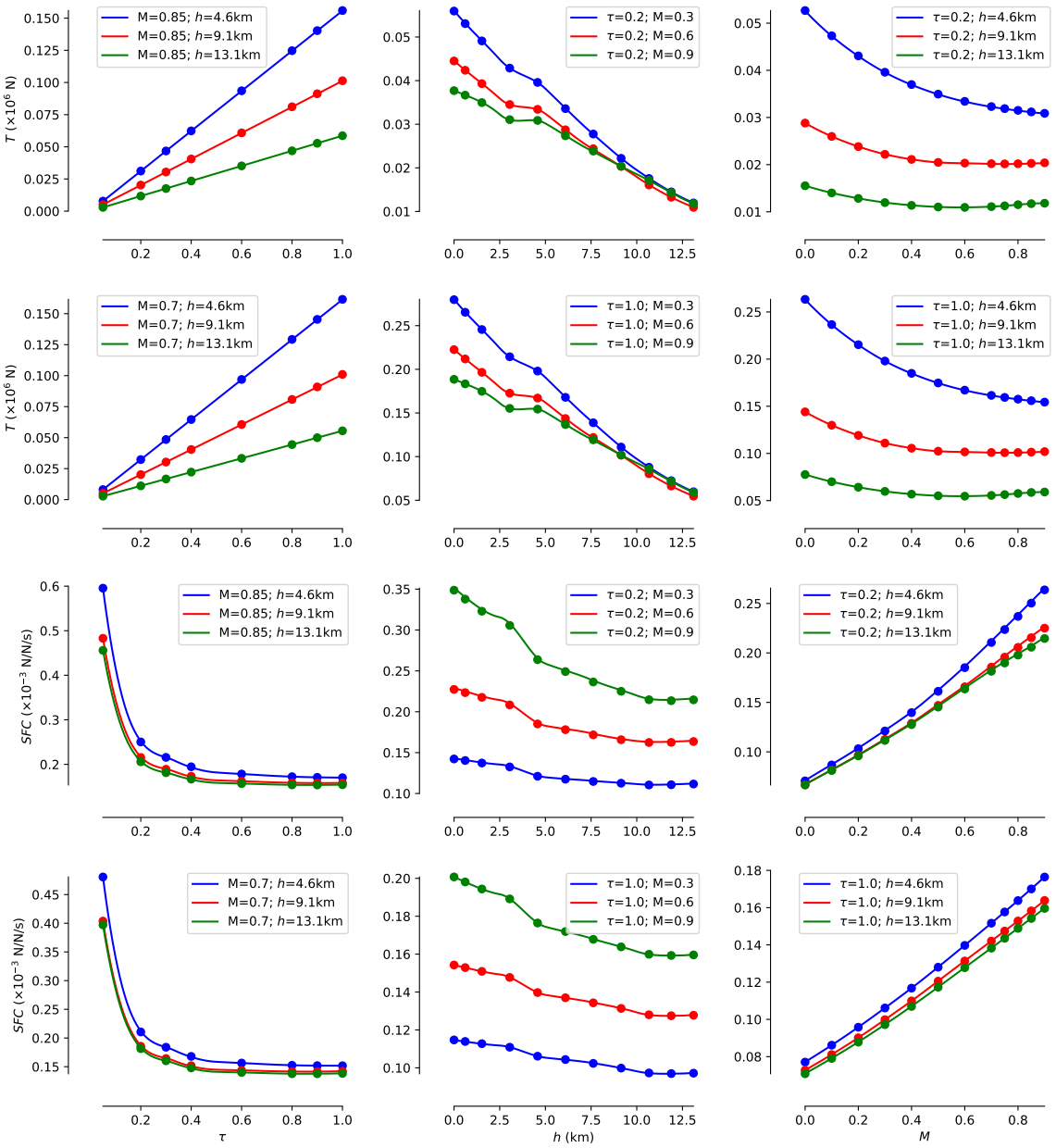

Figure 5: 1-D slices versus of thrust and specific fuel consumption versus throttle setting, altitude, and Mach number.

The fuel weight ODE is given by

$$\frac{dW_f}{dx} = \frac{\text{SFC} \cdot T}{v_x}, \tag{11}$$

where W_f is the fuel weight and x is the horizontal coordinate. This is an ODE because the right-hand side depends on W_f—W_f contributes to W, which affects L and thus D, which in turn affects T.

Incorporating an ODE in a model that is to be used for gradient-based optimization can be tricky because the equations for integrating the ODE must be differentiated. For this, we use a vectorized, parallel-in-time integration approach [55] using the general linear methods (GLM) formulation. Developing a differentiated ODE solver using GLMs enables rapid implementation of any Runge–Kutta or linear multistep ODE integrator with no need to derive and implement partial derivatives for each integrator [55]. We use this ODE solver, choosing the 2nd order Gauss–Legendre integrator based on the recommendations of a previous benchmarking study [55].

As we can see in Fig. 1, the mission analysis has a feedback loop. Fuel weight affects aircraft weight, which affects lift through the vertical equation of motion. Lift, in turn, affects drag through the aerodynamic surrogate model, and drag affects thrust through the horizontal equation of motion. Thrust can be mapped to SFC through the propulsion surrogate model, and SFC affects fuel weight through the ODE, completing the cycle. We found that in numerical experiments, the nonlinear block Gauss–Seidel iteration, which is essentially a fixed-point iteration, is the most efficient nonlinear solver, in the context of running a simulation. Likewise, we found the linear block Gauss–Seidel iteration to be the most efficient linear solver when computing derivatives.

4.7 Allocation problem equations

The allocation problem is formulated with two sets of design variables: the number of flights per day ($\text{flt}_{\text{day}_{i,j}}$) flown using each aircraft type j on each route i, and the corresponding number of passengers per flight ($\text{pax}_{\text{flt}_{i,j}}$). This formulation was first used as an application of linear programming in 1956 [19]. Here, we seek to maximize the profit subject to operational and demand constraints [36, 29].

The airline profit for a given number of routes (n_{rt}) and aircraft (n_{ac}) is evaluated using

$$\begin{aligned} \text{profit} = &\sum_{i}^{n_{rt}} \sum_{j}^{n_{ac}} \left[\text{price}_{\text{pax}_{i,j}} \cdot \text{pax}_{\text{flt}_{i,j}} \cdot \text{flt}_{\text{day}_{i,j}} \right] \\ &- \sum_{i}^{n_{rt}} \sum_{j}^{n_{ac}} \left[(\text{cost}_{\text{flt}_{i,j}} + \text{cost}_{\text{fuel}} \cdot \text{fuel}_{\text{flt}_{i,j}}) \cdot \text{flt}_{\text{day}_{i,j}} \right], \end{aligned} \tag{12}$$

where $\text{price}_{\text{pax}_{i,j}}$ is the ticket price per flight, $\text{cost}_{\text{flt}_{i,j}}$ is the total cost of operating a flight except for fuel costs, $\text{cost}_{\text{fuel}}$ is the assumed cost per unit fuel, and $\text{fuel}_{\text{flt}_{i,j}}$ is the total fuel burn for a flight.

The allocation problem contributes two inequality constraints to the optimization problem. The first inequality ensures that the total number of people that fly on a

given route on a given day is less than the total demand for that route and can be written as

$$\text{pax}_i = \sum_j^{n_{ac}} \left[\text{pax}_{\text{flt}_{i,j}} \cdot \text{flt}_{\text{day}_{i,j}} \right] \leq \text{demand}_i \ , \quad 1 \leq i \leq n_{rt}. \tag{13}$$

The second inequality constraint takes into consideration how many aircraft of a given type are actually owned by the airline and can be written as

$$\text{usage}_j = \sum_i^{n_{rt}} \left[\text{flt}_{\text{day}_{i,j}} \cdot \left(\text{time}_{\text{flt}_{i,j}} \left(1 + \text{maint}_j \right) + \text{turn}_{\text{flt}} \right) \right] \leq 12\text{hr} \cdot \text{num}_{ac_j} \ , \quad 1 \leq j \leq n_{ac}, \tag{14}$$

where $\text{time}_{\text{flt}_{i,j}}$ is the block time for a flight, maint_j is the maintenance time required as a multiple of block time, turn_{flt} is the turnaround time between flights, and num_{ac_j} is the number of aircraft available for type j.

5 Problem

As described in Sec. 3, we improve the optimization convergence by initializing the full MDO problem with the solution of three smaller optimization problems—design, mission, and allocation optimization. In this section, we describe each of the four optimization problems, which are all shown in Tab. 1.

Table 1: The optimization problem statements.

	Variable	Lower	Upper	Optimization problem (quantity)			
				Design	Mission	Allocation	Full
objective	drag (sum)			✓			
	fuel burn				✓		
	profit					✓	✓
design variables	wing area (rel.)	0.9	1.1	1			1
	wing sweep (deg)	−5	5	1			1
	wing twist (deg)	−8	8	7			7
	wing shape			192			192
	cruise Mach	0.6	0.865		1		1×128
	altitude (km)	0	13		20		20×128
	pax per flight	0	*			5×128	5×128
	flights per day	0	10			5×128	5×128
	total			201	21	1280	4169
constraints	wing LE/TE	0	0	2×8			2×8
	wing thickness (rel.)	0.5		25×30			25×30
	wing volume (rel.)	1.					
	wing C_m	−0.17		1			1
	climb angle (deg)	−20	20		100		100×128
	min. thrust (KS)	0.01			1		1×128
	max. thrust (KS)		1.00		1		1×128
	route demand	0	*			128	128
	aircraft count		*			5	5
	total			759	102	133	13921
problem type				NLP	NLP	MILP	NLP
optimizer				SNOPT	SNOPT	CPLEX	SNOPT

rel.: quantities that are relative to initial
NLP: nonlinear programming MILP: mixed-integer linear programming
SNOPT: optimizer for large-scale NLP problems CPLEX: optimizer package that includes LP, MILP solvers

5.1 Design problem

The geometry of interest is the common research model (CRM) wing, modeled with RANS CFD. The general properties of the aircraft are shown in Tab. 2 We use a roughly 50,000-cell mesh created using a hyperbolic mesh generation algorithm. We use a coarse mesh in order to minimize computation time and because detailed resolution of drag does not significantly affect our ability to evaluate the benefit of the allocation-mission-design optimization approach.

Table 2: Aircraft properties.

Reference area	419.0 m^2	4509.9 ft^2
Reference chord	7.8 m	25.7 ft
OEW	1.35×10^6 N	3.03×10^5 lb

The wing design variables consist of area, sweep, twist, and shape. The area change is constrained to be within 10% and sweep is constrained to vary by less than 5°. These restrictions are necessary because structural constraints and weights are not modeled. Our intent is to permit only small changes to overall aircraft sizing so that we can observe the general directions the optimization problem favors, such as a smaller or larger wing. As we see in Fig. 2, there are 8 sections of B-spline control points, so with the root fixed, there are 7 B-spline control points that parametrize the twist distribution. The shape design variables control the vertical component of the B-spline control points in Fig. 2. There are 8 sections with 24 control points per section, so there are 192 in total. The FFD volume uses 4th order B-splines.

There are 2×8 linear constraints for the leading and trailing edge of each section to ensure equal-and-opposite movement so that the shape variables do not add undesired twist. There are 750 thickness constraints, 25 span-wise and 30 chord-wise, for structural and manufacturing considerations as well as to prevent cross-over of the upper and lower surfaces. The thickness is constrained to be more than 50% of the original CRM thickness at each point. There is a constraint that the moment coefficient is at least -0.17, since we do not directly model trim drag, and this is applied at the nominal condition of $M = 0.85$ and $\alpha = 2°$. Finally, there is a volume constraint ensuring that the volume does not decrease below that of the CRM, for structural and fuel volume reasons. This constraint is scaled with area so that with a larger area, the minimum volume increases correspondingly, by $A^{\frac{3}{2}}$.

The design pre-optimization problem is as described in Tab. 1. It is a multipoint lift-constrained drag minimization with 9 equally-weighted points generated by a 3×3 grid formed from C_L values of $0.4, 0.5, 0.6$ and M values of $0.84, 0.85, 0.86$ at an altitude of 11 km (roughly 36,000 ft).

5.2 Mission problem

The mission problem has two groups of design variables—cruise Mach number and altitude control points. Cruise Mach number is constrained to be between 0.6 and 0.865, and with the altitude profile known, it uniquely determines the Mach number

profile over the mission using the relationship described in Sec. 4. The altitude profile is parametrized with a 4th order B-spline with 20 control points. Each mission, regardless of the range is discretized with 100 nodes.

There are three groups of constraints associated with the mission problem. There are linear constraints at each of the mission points constraining the climb angle to be between $-20°$ and $20°$. There are minimum and maximum thrust constraints that also apply at each mission point. However, since these are nonlinear and have derivatives that are expensive to compute, they are aggregated using Kreisselmeier–Steinhauser functions [53].

The mission pre-optimizations consists of 128 separate problems that minimize fuel burn for each of the 128 missions. From the design pre-optimization result, an aerodynamic surrogate model is generated once. This surrogate model is used in the 128 mission optimizations that generated initial values for the cruise Mach numbers and altitude control points for the full MDO problem.

5.3 Allocation problem

For the allocation problem, we use a hypothetical airline network with 128 routes, shown in Fig. 6. The routes range from roughly 400 km to 14000 km, and the allocation problem data, including the routes and the demand numbers, are obtained from the Fleet-Level Environmental Evaluation Tool (FLEET) developed at Purdue University [56]. The fleet is modeled after a quarter-size version of United Airlines' fleet, and is shown in Tab. 3. There are four types of existing aircraft, and a limited number of the aircraft being designed as well. The idea is that we are using optimization to determine the most profitable allocation of the next-generation aircraft we are designing (based on the CRM) in competition with the existing aircraft that the hypothetical airline has available.

Table 3: Aircraft fleet.

Aircraft	Quantity	Seat capacity
Embraer E-170	40	58
Boeing 737-800	42	122
Boeing 777-200ER	20	207
Boeing 747-400	5	294
Next-generation (CRM)	25	300

There are two groups of allocation design variables. The first is flights per day of each aircraft type (5) and route (128); there are 640 variables of this type. If the optimal value for route i and aircraft j is zero, we can interpret this as a result that it is not optimal to operate aircraft j on route i. The flights per day variable allows us to formulate the allocation problem in a continuous way that avoids representing the choice of route for each aircraft type using a discrete variable. The second allocation design variable is passengers per flight for each aircraft type and route, so there are 640 of these variables as well. This variable is necessary because when the passenger

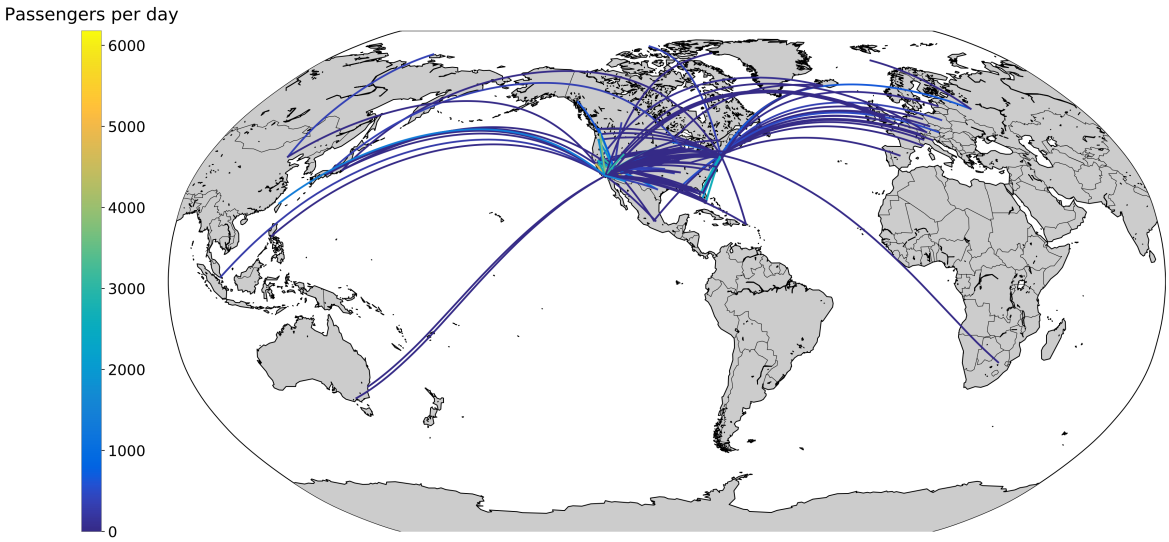

Figure 6: Visualization of the 128 routes. The color scale represents the total number of passengers flown on a given route per day.

demand constraint is active, at least one flight has the leftover number of passengers, rather than being full.

There are also two groups of allocation constraints. The passenger demand constraints limit the total number of passengers per day who fly on any aircraft for each route. Therefore, there are 128 such constraints, and they prevent the optimal allocation from excessively concentrating on a subset of routes that are the most profitable. The aircraft count constraints consider the total number of each type of aircraft that is available, the total flight times, the number of flights per day, and the hours per day that each can be flown. Therefore, this constraint captures the effect of having a finite fleet of aircraft with limited numbers of each type. In this work, we do not consider resource allocation aspects of airline operations such as crew scheduling and routing of individual aircraft, nor the times of specific flights.

The allocation pre-optimization optimizes the flights per day and passengers per flight variables given the fuel burn and block time values computed by the mission pre-optimizations. Since the fuel burn and block time values are fixed, this is a linear optimization problem that maximizes profit. The optimized flights per day and passengers per flight variables are used to initialize the corresponding values in the full MDO problem.

6 Results

In this section, we present the optimization results. We compare the AMD optimization results to the baseline, obtained by performing multipoint design optimization, then 128 separate mission optimizations, and then an allocation optimization. These are the same three optimization steps used to compute the initial values of the design variables for the AMD optimization. However, they also provide baseline values, because they

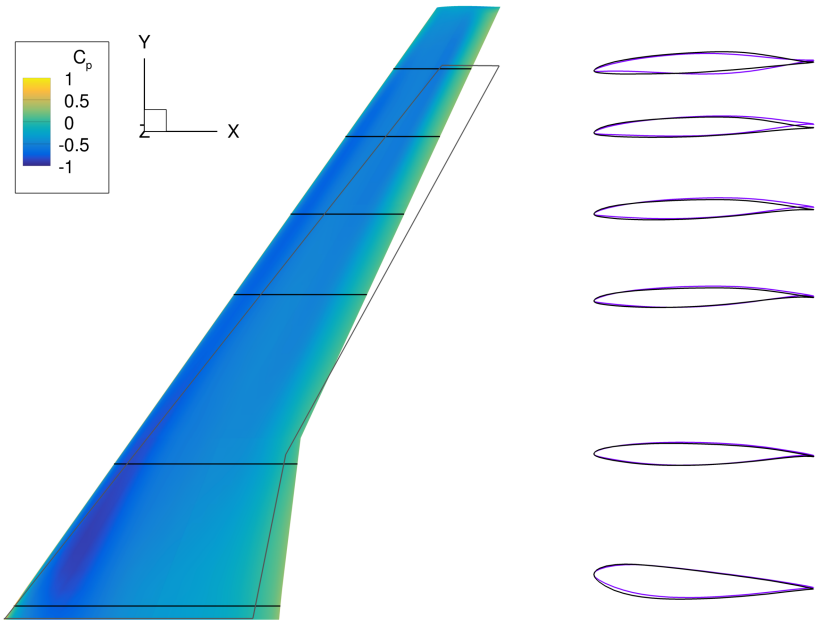

Figure 7: Initial (purple) and optimized (black) wing design. The grey outline depicts the planform for the initial wing.

represent the profit value corresponding to the multipoint-optimized design, assuming this design is flown with optimal mission profiles and with the optimal utilization within the airline.

6.1 Impact of simultaneous AMD optimization

The primary question we want to answer is whether the simultaneous allocation-mission-design optimization is worthwhile, compared to the conventional multipoint design optimization. To answer this question, we first look at the profit values resulting from the respective optimizations.

The AMD optimization results in an increase in profit from \$8.058 million per day to \$8.242 million per day, representing a 2.3% increase. We can interpret this result as follows—designing an aircraft using the AMD formulation and operating it in the way predicted by the AMD optimization yields a 2.3% higher profit compared to designing an aircraft using the multipoint formulation, which does not consider the actual operation, and then operating it optimally given the limits of this design. As we explore in the sections that follow, this increase in profit is achieved mostly through changes to the wing design and the mission profiles.

6.2 Wing design and performance

In Fig. 7, we show the wing design before and after AMD optimization. The initial wing design is the design that results from multipoint optimization.

The biggest difference we observe is an increase in wing area, which allows the

aircraft to cruise at its optimal lift-to-drag ratio at a higher altitude. A secondary effect is that increasing wing area increases chord, which in turn increases the Reynolds number, resulting in a lower viscous drag coefficient. The impact of wing area on structural weight is not considered here, which is why we put bounds on the area design variable to limit the change to 10%.

To first order, a 10% wing area increase leads to a similar percentage increase in wing structural weight. The weight of the wing ranges between 10–20% of the aircraft gross weight, so the increase in gross weight would be 1–3%. The gross weight is a first-order surrogate for aircraft acquisition cost, which in turn is on the order of 30% of flight operating cost. Therefore, the acquisition cost increase as a result of the larger wing would subtract, at worst, 1% from the 2.3% profit increase.

In terms of the airfoil shapes, we observe that the AMD optimum has a more blunt leading edge. This is consistent with what is observed in multipoint optimization because the AMD optimization considers a wider range of operating conditions that suppress the sharper leading edges characteristic of airfoils designed for a narrow range of conditions.

We also observe a decrease in wing sweep, which results in more lift, but also more wave drag and less pitch-up moment for satisfying the moment constraint. Similarly, we observe a decrease in washout in the AMD-optimized wing. Both the wing sweep and washout decrease because with a larger wing at lower angle of attack, the pitch-down moment that must be counteracted is smaller.

In Fig. 8, we show contours of lift-to-drag ratio versus lift coefficient and Mach number for the initial and optimized wing designs with the $L/D = 26$ contour highlighted in grey. The 36 training points are shown with red markers (only 18 are clearly visible because there are two slices in the altitude dimension), and the path of the longest-range mission is shown in black. First, we observe that the AMD-optimized design flies at higher Mach numbers—this is due to the previously-described Mach schedule that we assume, combined with the increases in the altitude profiles. Second, we observe that the region where $L/D > 26$ shrinks and the AMD optimization result is less aerodynamically efficient; however, this is offset by the increase in propulsive efficiency as we will see later.

6.3 Mission design

We now consider the impact of the AMD optimization in terms of the optimized mission profiles. In Fig. 9, we show the altitude profiles for the CRM on all 128 routes with the inactive routes (those on which the CRM has 0 flights per day) shown in grey. As discussed previously, we observe that the optimal cruise-climb altitudes increase after the AMD optimization, while the altitude profiles in grey do not change, as expected. The altitude increase is related to the increase in wing area as the larger wing offsets the reduction in density at higher altitudes, while maintaining the optimal L/D. Increasing altitude also decreases specific fuel consumption, and decreases thrust, forcing an increase in throttle, which also decreases specific fuel consumption. This coupling between aerodynamics, propulsion, and mission analysis is not captured by

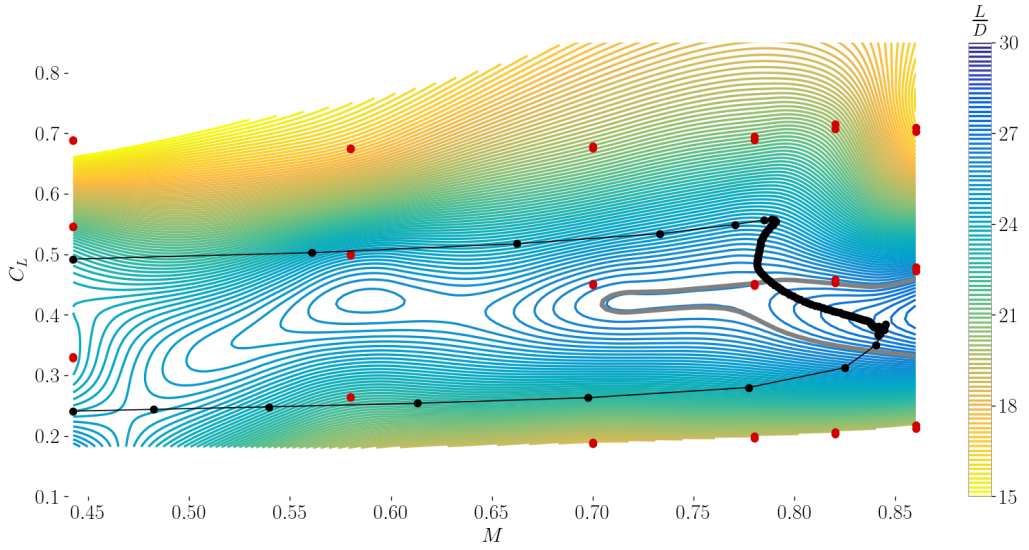

Initial design

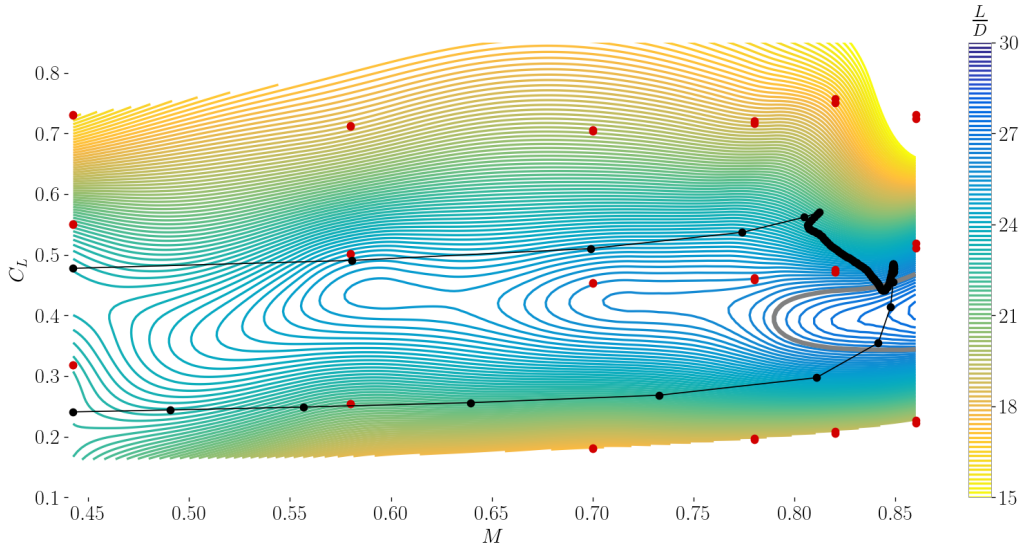

Optimized design

Figure 8: The contours show L/D, the red markers indicate training point locations, and the black markers and lines indicate the path of the aircraft through C_L-M space for the longest-range mission. The $L/D = 26$ contour is highlighted in grey.

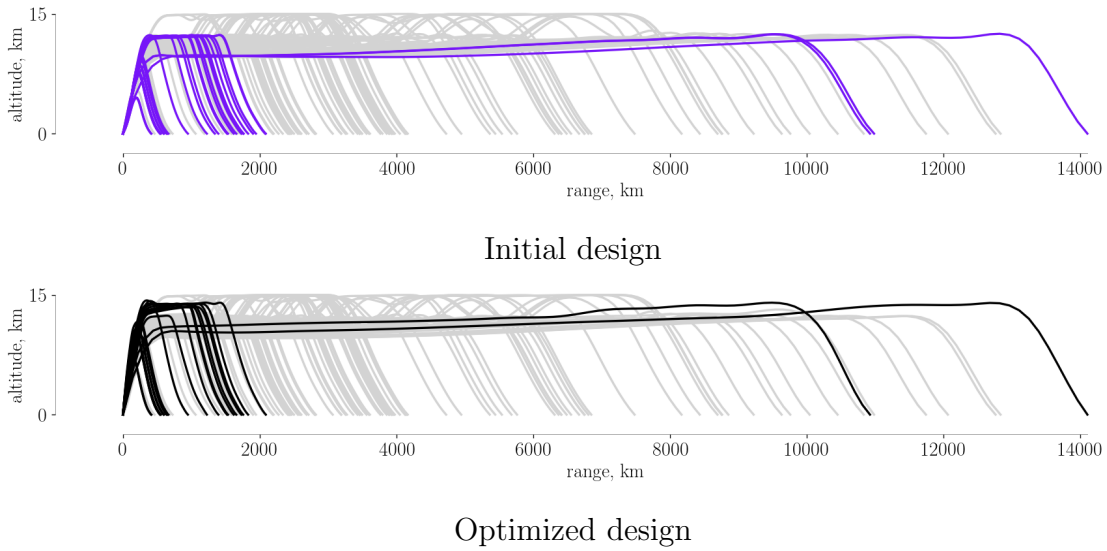

Figure 9: The altitude profiles for: routes on which the CRM is not flown (grey), the initial design (purple), and the optimized design (black).

the multipoint optimization formulation—wing area is sized purely for aerodynamic considerations, but increased propulsive efficiency via an increase in altitude is another motivation for increasing wing area.

We note that the optimized altitude at the start of cruise is approximately the same, regardless of the mission. This is expected because the optimal altitude is a function of the aircraft weight at a given operating condition. The aircraft has roughly the same amount of fuel remaining to start the descent regardless of the range, so the altitude just prior to descent should be the same across all routes, and we see this in the optimization results.

In Fig. 10, we show the relative changes in fuel burn and block time for each route due to the AMD optimization. The fuel burn decreases in all but the shortest routes, and the decrease is larger for longer routes. We hypothesize that this is because most of the reduction in fuel burn comes from the increase in propulsive efficiency during cruise which is a small proportion of the mission for short-haul routes.

The reduction in block times can be attributed to two factors. First, the Mach number profiles are higher overall for all routes because of the higher altitudes combined with the Mach schedule that we assume. Second, the cruise Mach number is not at the maximum of 0.85 in the baseline mission optimization results, but they increase to the upper bound after the AMD optimization. This is because the AMD optimization rewards flying faster with a greater utilization rate for the airline. When optimizing the design, then mission, then allocation, this feedback from the allocation problem to the mission optimization problem is not captured.

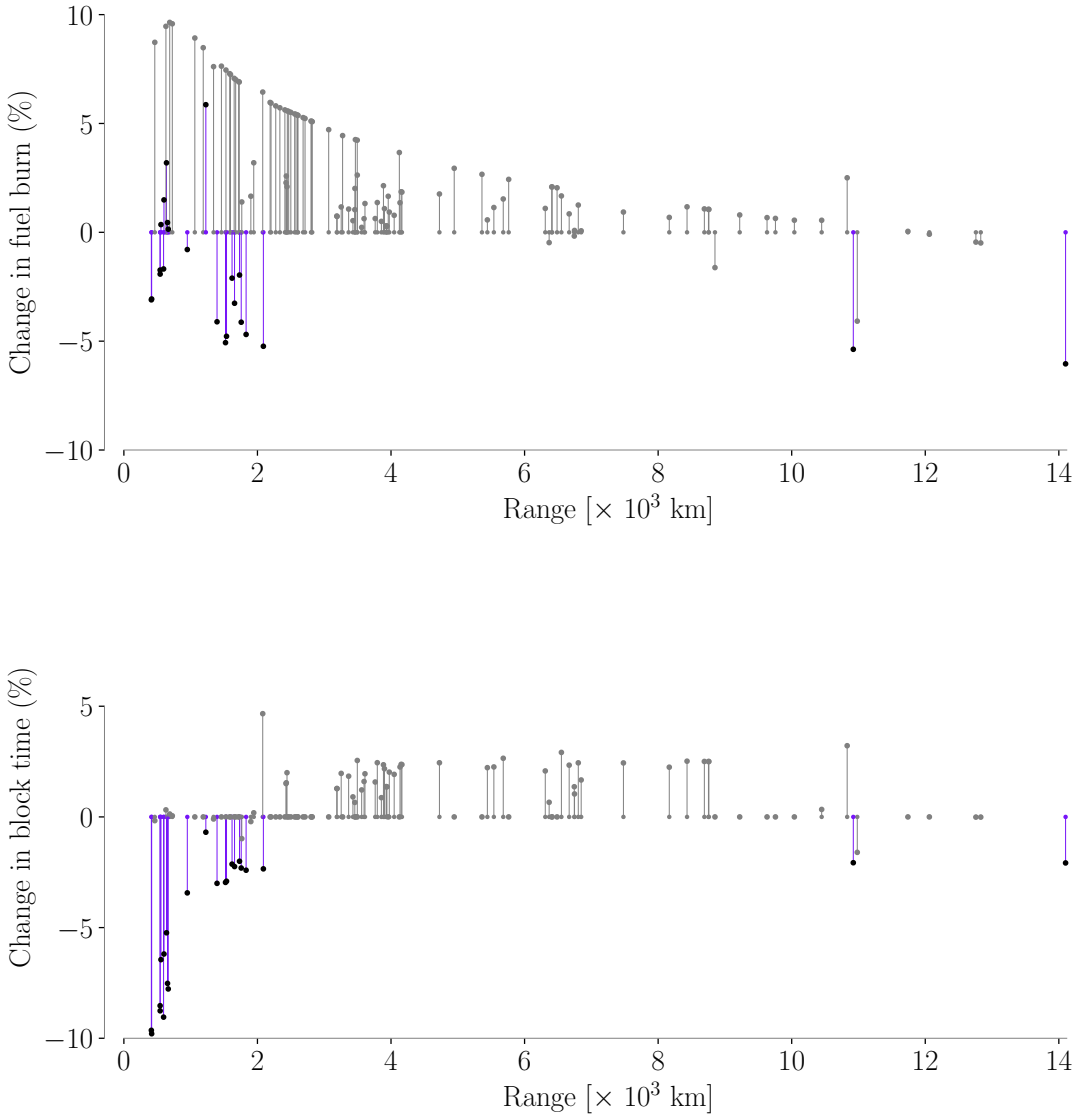

Figure 10: Missions on which the CRM is not flown are in grey, values for the initial design are in purple, and values for the optimized design are in black.

6.4 Allocation problem

In Fig. 11, we show the total number of passengers flown daily for each aircraft type and for each route. This is the result of multiplying the flights per day and passengers per flight design variables. We observe small changes in the utilization of the CRM and none for the other aircraft types—this is expected since we perform design and mission optimization for only the CRM. However, a major reason for the small changes in the allocation is that the sizing for the CRM is largely fixed and the number of seats is not allowed to change. This prevents us from making conclusive statements regarding the strength of the design-allocation coupling with respect to the fleet allocation design variables. If larger-scale design changes were permitted, a larger change in the allocation would be expected.

Since we are using a gradient-based optimization approach, we can expect the AMD solution to be dependent on the initial values computed by the pre-optimizations. For the allocation variables, this can be an advantage because the allocation-only pre-optimization solves a linear problem that does not have multiple local minima. Therefore, it computes the global solution to the allocation problem within the assumptions of the linear problem. In future work, using the AMD solution to update the inputs to the allocation-only pre-optimization and running a second cycle of pre-optimizations and then the AMD optimization would provide more confidence in the global optimality of the final solution.

7 Conclusion

We presented in this paper an algorithm that performs high-fidelity aircraft design optimization using CFD while simultaneously optimizing the mission profiles and airline allocation. We solve a single monolithic optimization problem in which the design variables include: the area, sweep, shape, and twist distribution of a common research model wing; the cruise Mach number and altitude profile for the aircraft's trajectory on 128 candidate routes; and the number of flights per day and passengers flight for each route and each of several types of aircraft that the hypothetical airline owns. We maximize profit for this hypothetical airline that operates 128 routes with a set of existing aircraft and a finite number of the new aircraft being designed.

To enable this formulation, we use gradient-based optimization and develop an approach in which a surrogate model for the CFD is trained in each optimization iteration in terms of angle of attack, Mach number, and altitude. We use this surrogate model to perform the analysis of the discretized mission for each of the 128 routes. The surrogate modeling approach is unique because it includes derivatives of the prediction outputs with respect to the training data outputs, which are needed for the dynamic retraining. The profit and relevant constraints from the airline allocation problem are computed using simple formulas.

The complexity of the multidisciplinary model and of the derivative computation is mitigated by using the modular analysis and unified derivatives (MAUD) architecture, which is the approach of constructing the model is a particular, modular way and

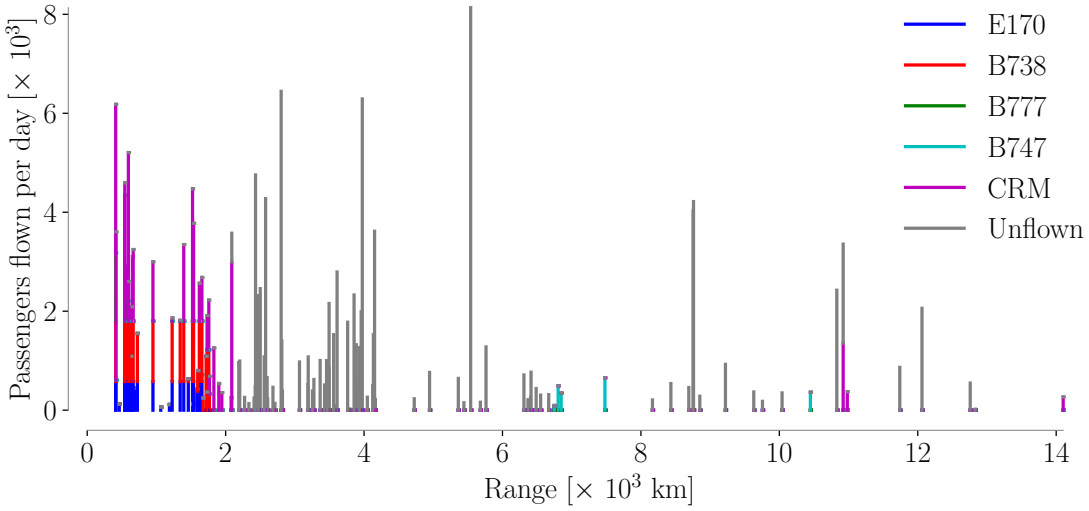

Initial design

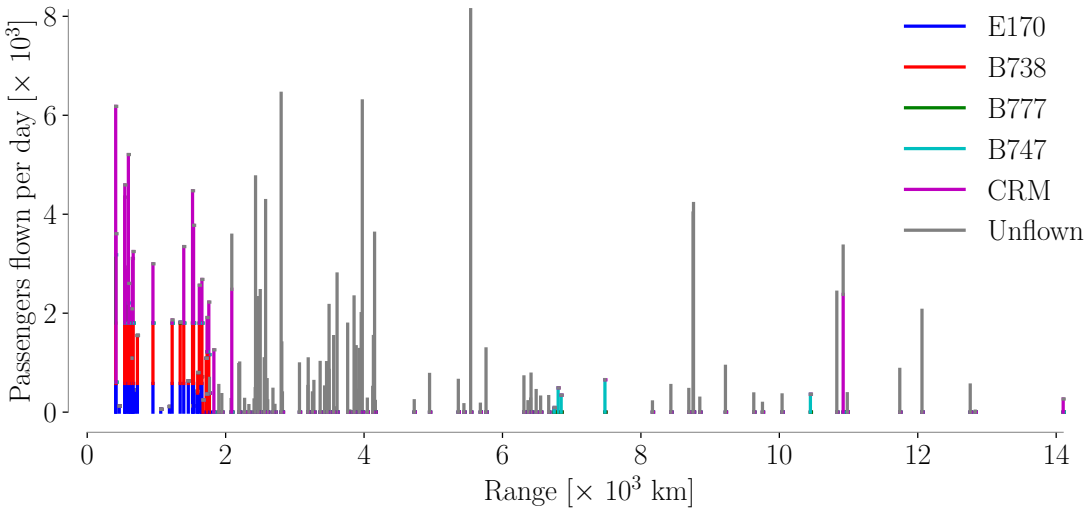

Optimized design

Figure 11: Total number of passengers flown per day for each aircraft type and for each route.

performing adjoint derivative computation using a unified equation. We develop our model within the OpenMDAO framework, which implements the MAUD architecture. MAUD recasts the derivative computation problem into the solution of a linear system, and it facilitates the use of parallel computing in executing the model and computing the derivatives. In this problem, we parallelize in three ways—across the CFD training points, within each CFD training point, and across the 128 mission analyses.

The allocation-mission-design (AMD) optimization problem is solved and compared to the traditional approach for CFD-based shape optimization, which is multipoint optimization. We follow the multipoint optimization with 128 decoupled mission optimizations and an allocation-only optimization, to obtain initial design variables values for the AMD optimization and to provide a baseline profit value. Compared to this baseline, the AMD optimization results in a 2.3% increase in daily profit for the hypothetical airline, from \$8.058 million to \$8.242 million. The wing area increases by 10%, enabling the aircraft to cruise at a higher altitude with a similar lift-to-drag ratio, which in turn leads to improvements in propulsive efficiency. The airline profit increase is thus achieved through a combination of reduced fuel burns for each mission and reduced block times, which enables the airline to operate more flights. The largest change is for a flight of about 11,000 km, where the number of flights per day increases by just over 3 flights.

We draw two main conclusions from this research effort. First, we have quantified the benefit of performing high-fidelity design optimization with mission and allocation optimization in the same problem to be 2.3% in airline profit for our problem, given the limitations of our approach. The wing design that results is different (10% larger area) from that from the traditional multipoint optimization, and the latter is predicted to cause the aforementioned loss of profit. Our second conclusion is that the coupling between design, mission, and allocation is significant in the sense that the optimal design is very different when optimized for profit, rather than when using a multipoint fuel-burn objective. The wing area affects not only the aerodynamic performance but also the mission analysis and thus the propulsive efficiency because it affects the cruise altitude, which has a strong impact on specific fuel consumption. Therefore, the aerodynamics and propulsion should be modeled together along with the full mission profile, and this motivates the inclusion of the allocation problem because many long-haul aircraft have historically spent a significant portion of their operation in short-haul routes.

The most significant limitation of this study is the exclusion of structures and weights, which prevents the algorithm from capturing important design trades affecting wing area and sweep. A second limitation is the fact that it permits non-integer numbers of flights per day in order to keep the optimization problem non-discrete. Another major limitation is not considering high-lift configurations, which contributes non-trivial error for short-range routes. However, these limitations can be overcome with more accurate models and greater computational power, and they do not detract from the method developed in the paper for optimizing the design, mission, and allocation simultaneously. In addition to addressing these limitations, the most relevant area for future work is the application of this technique to the design of unconventional configurations with sufficient fidelity to allow for non-trivial changes in aircraft

sizing—where the difference between the AMD optimization and a traditional multipoint optimization is expected to be much larger.

8 Acknowledgments

The authors gratefully acknowledge support from NASA through grant number NNX14AC73A (technical monitor: Tristan Hearn). The first author was partially supported by the NASA ARMD Transformational Tools and Technologies Project. The second author is grateful for support from the National Science Foundation Graduate Research Fellowship under Grant No. DGE-1256260. The authors also thank Satadru Roy for providing the data for the airline allocation problem.

A Temperature smoothing function coefficients

$$\begin{bmatrix} (h_t-\epsilon)^3 & (h_t-\epsilon)^2 & (h_t-\epsilon) & 1 \\ (h_t+\epsilon)^3 & (h_t+\epsilon)^2 & (h_t+\epsilon) & 1 \\ 3(h_t-\epsilon)^2 & 2(h_t-\epsilon) & 1 & 0 \\ 3(h_t+\epsilon)^2 & 2(h_t+\epsilon) & 1 & 0 \end{bmatrix} \begin{bmatrix} c_3 \\ c_2 \\ c_1 \\ c_0 \end{bmatrix} = \begin{bmatrix} T_0 - L \times (h_t-\epsilon) \\ T_2 \\ -L \\ 0 \end{bmatrix} \tag{15}$$

B Pressure smoothing function coefficients

$$\begin{bmatrix} (h_t-\epsilon)^3 & (h_t-\epsilon)^2 & (h_t-\epsilon) & 1 \\ (h_t+\epsilon)^3 & (h_t+\epsilon)^2 & (h_t+\epsilon) & 1 \\ 3(h_t-\epsilon)^2 & 2(h_t-\epsilon) & 1 & 0 \\ 3(h_t+\epsilon)^2 & 2(h_t+\epsilon) & 1 & 0 \end{bmatrix} \begin{bmatrix} d_3 \\ d_2 \\ d_1 \\ d_0 \end{bmatrix} = \begin{bmatrix} p_0 \left(\frac{T(h_t-\epsilon)}{T_0}\right)^{\frac{g}{LR}} \\ p_1 \exp\left(-\frac{g\epsilon}{RT_1}\right) \\ -\frac{gp_0}{R}\left(\frac{T(h_t-\epsilon)}{T_0}\right)^{\frac{g}{LR}-1} \\ \frac{-gp_1}{RT_1}\exp\left(\frac{g(-\epsilon)}{RT_1}\right) \end{bmatrix} \tag{16}$$

References

[1] Del Rosario, R., Follen, G., Wahls, R., and Madavan, N., "Subsonic Fixed Wing Project Overview of Technical Challenges for Energy Efficient, Environmentally Compatible Subsonic Transport Aircraft," *Proceedings of the 50th AIAA Aerospace Sciences Meeting*, Nashville, TN, 2012.

[2] Kenway, G. K. W., Kennedy, G. J., and Martins, J. R. R. A., "Scalable Parallel Approach for High-Fidelity Steady-State Aeroelastic Analysis and Derivative Computations," *AIAA Journal*, Vol. 52, No. 5, May 2014, pp. 935–951. doi:10.2514/1.J052255.

[3] Kenway, G. K. W. and Martins, J. R. R. A., "Multipoint High-Fidelity Aerostructural Optimization of a Transport Aircraft Configuration," *Journal of Aircraft*, Vol. 51, No. 1, January 2014, pp. 144–160. doi:10.2514/1.C032150.

[4] Lyu, Z. and Martins, J. R. R. A., "Aerodynamic Design Optimization Studies of a Blended-Wing-Body Aircraft," *Journal of Aircraft*, Vol. 51, No. 5, September 2014, pp. 1604–1617. doi:10.2514/1.C032491.

[5] Secco, N. R. and Martins, J. R. R. A., "RANS-based Aerodynamic Shape Optimization of a Strut-braced Wing with Overset Meshes," *Journal of Aircraft*, Vol. 56, No. 1, January 2019, pp. 217–227. doi:10.2514/1.C034934.

[6] Mader, C. A., Kenway, G. K., Martins, J., and Uranga, A., "Aerostructural Optimization of the D8 Wing with Varying Cruise Mach Numbers," *18th AIAA/ISSMO Multidisciplinary Analysis and Optimization Conference*, Denver, CO, 2017, AIAA 2017–4436.

[7] Casey, D., "Boeing 787 Dreamliner - Q3 update," `https://www.routesonline.com/news/29/breaking-news/274180/boeing-787-dreamliner-q3-update/`, 2017, Accessed: 2017-12-20.

[8] Vassberg, J. C., DeHaan, M. A., Rivers, S. M., and Wahls, R. A., "Development of a Common Research Model for Applied CFD Validation Studies," 2008. doi:10.2514/6.2008-6919, AIAA 2008-6919.

[9] Hwang, J. T. and Martins, J., "Allocation-mission-design optimization of next-generation aircraft using a parallel computational framework," *57th AIAA/ASCE/AHS/ASC Structures, Structural Dynamics, and Materials Conference*, 2016, AIAA 2016–1662.

[10] Mane, M. and Crossley, W. A., "Allocation and design of aircraft for on-demand air transportation with uncertain operations," *Journal of aircraft*, Vol. 49, No. 1, 2012, pp. 141–150.

[11] Haug, E. J. and Arora, J. S., "Design sensitivity analysis of elastic mechanical systems," *Computer Methods in Applied Mechanics and Engineering*, Vol. 15, No. 1, 1978, pp. 35–62.

[12] Drela, M., "Pros and cons of airfoil optimization," *Frontiers of Computational Fluid Dynamics*, 1998, pp. 363–381.

[13] Li, W., Huyse, L., and Padula, S., "Robust airfoil optimization to achieve drag reduction over a range of mach numbers," *Structural and Multidisciplinary Optimization*, Vol. 24, No. 1, 2002, pp. 38–50.

[14] Brooks, T. R., Kenway, G. K. W., and Martins, J. R. R. A., "Benchmark Aerostructural Models for the Study of Transonic Aircraft Wings," *AIAA Journal*, Vol. 56, No. 7, July 2018, pp. 2840–2855. doi:10.2514/1.J056603.

[15] Burdette, D. A. and Martins, J. R. R. A., "Impact of Morphing Trailing Edge on Mission Performance for the Common Research Model," *Journal of Aircraft*, Vol. 56, No. 1, January 2019, pp. 369–384. doi:10.2514/1.C034967.

[16] Burdette, D. and Martins, J. R. R. A., "Design of a Transonic Wing with an Adaptive Morphing Trailing Edge via Aerostructural Optimization," *Aerospace Science and Technology*, Vol. 81, October 2018, pp. 192–203. doi:10.1016/j.ast.2018.08.004.

[17] Brooks, T. R., Kennedy, G. J., and Martins, J. R. R. A., "High-fidelity Multipoint Aerostructural Optimization of a High Aspect Ratio Tow-steered Composite Wing," *Proceedings of the 58th AIAA/ASCE/AHS/ASC Structures, Structural Dynamics, and Materials Conference, AIAA SciTech Forum*, Grapevine, TX, January 2017. doi:10.2514/6.2017-1350.

[18] Liem, R. P., Kenway, G. K., and Martins, J. R. R. A., "Multi-point, multi-mission, high-fidelity aerostructural optimization of a long-range aircraft configuration," *Proceedings of the 14th AIAA/ISSMO Multidisciplinary Analysis and Optimization Conference*, Indianapolis, IN, Sept. 2012. doi:10.2514/6.2012-5706.

[19] Ferguson, A. R. and Dantzig, G. B., "The allocation of aircraft to routes—An example of linear programming under uncertain demand," *Management science*, Vol. 3, No. 1, 1956, pp. 45–73.

[20] Gass, S., "George B. Dantzig," *Profiles in Operations Research*, edited by A. A. Assad and S. I. Gass, Vol. 147 of *International Series in Operations Research & Management Science*, Springer US, 2011, pp. 217–240. doi:10.1007/978-1-4419-6281-2_13.

[21] Simpson, R. W., *Computerized schedule construction for an airline transportation system*, Massachusetts Institute of Technology, 1966.

[22] Abara, J., "Applying integer linear programming to the fleet assignment problem," *Interfaces*, Vol. 19, No. 4, 1989, pp. 20–28.

[23] Barnhart, C., Farahat, A., and Lohatepanont, M., "Airline fleet assignment with enhanced revenue modeling," *Operations research*, Vol. 57, No. 1, 2009, pp. 231–244.

[24] Dumas, J., Aithnard, F., and Soumis, F., "Improving the objective function of the fleet assignment problem," *Transportation Research Part B: Methodological*, Vol. 43, No. 4, 2009, pp. 466–475.

[25] Lohatepanont, M. and Barnhart, C., "Airline schedule planning: Integrated models and algorithms for schedule design and fleet assignment," *Transportation Science*, Vol. 38, No. 1, 2004, pp. 19–32.

[26] Subramanian, R., Scheff, R. P., Quillinan, J. D., Wiper, D. S., and Marsten, R. E., "Coldstart: fleet assignment at delta air lines," *Interfaces*, Vol. 24, No. 1, 1994, pp. 104–120.

[27] Kontogiorgis, S. and Acharya, S., "US Airways automates its weekend fleet assignment," *Interfaces*, Vol. 29, No. 3, 1999, pp. 52–62.

[28] Mane, M., Crossley, W. A., and Nusawardhana, A., "System-of-systems inspired aircraft sizing and airline resource allocation via decomposition," *Journal of aircraft*, Vol. 44, No. 4, 2007, pp. 1222–1235.

[29] Govindaraju, P. and Crossley, W. A., "Profit motivated airline fleet allocation and concurrent aircraft design for multiple airlines," *2013 Aviation Technology, Integration, and Operations Conference*, 2013, AIAA 2013–4391.

[30] Marwaha, G. and Kokkolaras, M., "System-of-systems approach to air transportation design using nested optimization and direct search," *Structural and Multidisciplinary Optimization*, Vol. 51, No. 4, 2015, pp. 885–901.

[31] Roy, S. and Crossley, W. A., "An EGO-like Optimization Framework for Simultaneous Aircraft Design and Airline Allocation," *57th AIAA/ASCE/AHS/ASC Structures, Structural Dynamics, and Materials Conference*, 2016, AIAA 2016–1659.

[32] Roy, S., Moore, K., Hwang, J. T., Gray, J. S., Crossley, W. A., and Martins, J., "A mixed integer efficient global optimization algorithm for the simultaneous aircraft allocation-mission-design problem," *58th AIAA/ASCE/AHS/ASC Structures, Structural Dynamics, and Materials Conference*, 2017, AIAA 2017–1305.

[33] Roy, S., *A Mixed Integer Efficient Global Optimization Framework: Applied to the Simultaneous Aircraft Design, Airline Allocation and Revenue Management Problem*, Ph.D. thesis, Purdue University, 2017.

[34] Jansen, P. W. and Perez, R. E., "Robust Coupled Optimization of Aircraft Design and Fleet Allocation for Multiple Markets," *AIAA/3AF Aircraft Noise and Emissions Reduction Symposium*, 2014, AIAA 2014–2735.

[35] Jansen, P. W. and Perez, R. E., "Coupled optimization of aircraft families and fleet allocation for multiple markets," *Journal of Aircraft*, Vol. 53, No. 5, 2016, pp. 1485–1504.

[36] Hwang, J. T., Roy, S., Kao, J. Y., Martins, J., and Crossley, W. A., "Simultaneous aircraft allocation and mission optimization using a modular adjoint approach," *Proceedings of the 56th AIAA/ASCE/AHS/ASC Structures, Structural Dynamics and Materials Conference*, 2015, AIAA 2015–0900.

[37] Hwang, J. T. and Martins, J., "Parallel allocation-mission optimization of a 128-route network," *16th AIAA/ISSMO Multidisciplinary Analysis and Optimization Conference*, 2015, AIAA 2015–2321.

[38] Lambe, A. B. and Martins, J. R. R. A., "Extensions to the Design Structure Matrix for the Description of Multidisciplinary Design, Analysis, and Optimization Processes," *Structural and Multidisciplinary Optimization*, Vol. 46, August 2012, pp. 273–284. doi:10.1007/s00158-012-0763-y.

[39] Martins, J. R. R. A. and Lambe, A. B., "Multidisciplinary Design Optimization: A Survey of Architectures," *AIAA Journal*, Vol. 51, No. 9, September 2013, pp. 2049–2075. doi:10.2514/1.J051895.

[40] Cramer, E. J., Dennis, J. E., Frank, P. D., Lewis, R. M., and Shubin, G. R., "Problem Formulation for Multidisciplinary Optimization," *SIAM Journal on Optimization*, Vol. 4, No. 4, 1994, pp. 754–776.

[41] Gill, P. E., Murray, W., and Saunders, M. A., "An SQP algorithm for large-scale constrained optimization," *Society for Industrial and Applied Mathematics*, Vol. 47, No. 1, 2005.

[42] Mader, C. A., Martins, J. R. R. A., Alonso, J. J., and van der Weide, E., "ADjoint: An Approach for the Rapid Development of Discrete Adjoint Solvers," *AIAA Journal*, Vol. 46, No. 4, April 2008, pp. 863–873. doi:10.2514/1.29123.

[43] Lyu, Z., Kenway, G. K., Paige, C., and Martins, J. R. R. A., "Automatic Differentiation Adjoint of the Reynolds-Averaged Navier–Stokes Equations with a Turbulence Model," *21st AIAA Computational Fluid Dynamics Conference*, San Diego, CA, July 2013. doi:10.2514/6.2013-2581.

[44] Gray, J., Hearn, T., Moore, K., Hwang, J. T., Martins, J. R. R. A., and Ning, A., "Automatic Evaluation of Multidisciplinary Derivatives Using a Graph-Based Problem Formulation in OpenMDAO," *Proceedings of the 15th AIAA/ISSMO Multidisciplinary Analysis and Optimization Conference*, Atlanta, GA, June 2014. doi:10.2514/6.2014-2042.

[45] Hwang, J. T. and Martins, J. R. R. A., "A computational architecture for coupling heterogeneous numerical models and computing coupled derivatives," *ACM Transactions on Mathematical Software*, Vol. 44, No. 4, June 2018, pp. Article 37. doi:10.1145/3182393.

[46] Martins, J. R. R. A., Alonso, J. J., and Reuther, J. J., "A Coupled-Adjoint Sensitivity Analysis Method for High-Fidelity Aero-Structural Design," *Optimization and Engineering*, Vol. 6, No. 1, March 2005, pp. 33–62. doi:10.1023/B:OPTE.0000048536.47956.62.

[47] Martins, J. R. R. A. and Hwang, J. T., "Review and Unification of Methods for Computing Derivatives of Multidisciplinary Computational Models," *AIAA Journal*, Vol. 51, No. 11, November 2013, pp. 2582–2599. doi:10.2514/1.J052184.

[48] Hwang, J. T. and Martins, J. R. R. A., "A fast-prediction surrogate model for large datasets," *Aerospace Science and Technology*, Vol. 75, 2018, pp. 74 – 87. doi:10.1016/j.ast.2017.12.030.

[49] Lyu, Z., Kenway, G. K. W., and Martins, J. R. R. A., "Aerodynamic Shape Optimization Investigations of the Common Research Model Wing Benchmark," *AIAA Journal*, Vol. 53, No. 4, April 2015, pp. 968–985. doi:10.2514/1.J053318.

[50] Martins, J. R. R. A., Sturdza, P., and Alonso, J. J., "The Complex-Step Derivative Approximation," *ACM Transactions on Mathematical Software*, Vol. 29, No. 3, September 2003, pp. 245–262. doi:10.1145/838250.838251.

[51] Lyu, Z., *High-Fidelity Aerodynamic Design Optimization of Aircraft Configurations*, Ph.D. thesis, University of Michigan, 2014.

[52] Uyttersprot, L., *Inverse Distance Weighting Mesh Deformation*, Ph.D. thesis, Delft University of Technology, 2014.

[53] Kreisselmeier, G. and Steinhauser, R., "Systematic Control Design by Optimizing a Vector Performance Index," *International Federation of Active Controls Symposium on Computer-Aided Design of Control Systems, Zurich, Switzerland*, 1979. doi:10.1016/S1474-6670(17)65584-8.

[54] Claus, R. W., Evans, A., Lylte, J., and Nichols, L., "Numerical propulsion system simulation," *Computing Systems in Engineering*, Vol. 2, No. 4, 1991, pp. 357–364.

[55] Hwang, J. T. and Munster, D. W., "Solution of ordinary differential equations in gradient-basedmultidisciplinary design optimization," *2018 AIAA/ASCE/AHS/ASC Structures, Structural Dynamics, and Materials Conference*, Orlando, FL, January 2018.

[56] Moolchandani, K., Govindaraju, P., Roy, S., Crossley, W. A., and DeLaurentis, D. A., "Assessing effects of aircraft and fuel technology advancement on select aviation environmental impacts," *Journal of Aircraft*, Vol. 54, No. 3, 2016, pp. 857–869.